2/10/98
ORIGINAL

Closed-loop Control of Functional Neuromuscular Stimulation

NIH Neuroprosthesis Program Contract Number N01-NS-6-2338
Quarterly Progress Report #7
October 1, 1997 to December 31, 1997

Investigators:
Patrick E. Crago, Ph.D.
Clayton L. Van Doren, Ph.D.
Warren M. Grill, Ph.D.
Michael W. Keith, M.D.
Kevin L. Kilgore, Ph.D.
Joseph M. Mansour, Ph.D.
P. Hunter Peckham, Ph.D.
David L. Wilson, Ph.D.

Departments of
Biomedical Engineering,
Mechanical and Aerospace Engineering,
and Orthopaedics
Case Western Reserve University
and MetroHealth Medical Center

THIS QPR IS BEING SENT TO YOU BEFORE IT HAS BEEN REVIEWED BY THE STAFF OF THE NEURAL PROSTHESIS PROGRAM.

TABLE OF CONTENTS ERROR! BOOKMARK NOT DEFINED.

1. SYNTHESIS OF UPPER EXTREMITY FUNCTION

The overall goals of this project are (1) to measure the biomechanical properties of the neuroprosthesis user's upper extremity and incorporate those measurements into a complete model with robust predictive capability, and (2) to use the predictions of the model to improve the grasp output of the hand neuroprosthesis for individual users.

1. a. BIOMECHANICAL MODELING: PARAMETERIZATION AND VALIDATION

Purpose

In this section of the contract, we will develop methods for obtaining biomechanical data from individual persons. Individualized data will form the basis for model-assisted implementation of upper extremity FNS. Using individualized biomechanical models, specific treatment procedures will be evaluated for individuals The person-specific parameters of interest are tendon moment arms and lines of action, passive moments, and maximum active joint moments. Passive moments will be decomposed into components arising from stiffness inherent to a joint and from passive stretching of muscle-tendon units that cross one or more joints.

Report of progress

1. a. i. MOMENT ARMS VIA MAGNETIC RESONANCE IMAGING

Abstract

In this quarter, we continued the analysis of the moment arm of the flexor digitorum profundus at the third metacarpophalangeal (MCP) joint. We developed some new analysis techniques for examining image data. We discovered image evidence demonstrating that the tendon moment arm increases because the tendon moves toward the palmar surface and the joint center of rotation moves toward the dorsal surface of the hand. From a single set of image data analyzed by 3 operators, it was discovered that the precision of the 3D tendon excursion method was much less affected by segmentation error and operator subjectivity than the 3D geometric method. Because of significant differences in moment arm from one subject to another and because moment arm increased with flexion, we recommend patient-specific measurements for target applications in functional neuromuscular stimulation interventions and tendon transfer surgery.

Progress Report

In the last quarter, the 3 methods for evaluating tendon moment arm were compared on 4 subjects each measured 2 times. The three methods were: (1) a 3D tendon excursion method that extended the method of Landsmeer, (2) a 3D geometric method whereby the moment arm was the shortest distance between the joint axis of rotation and the tendon path, and (3) a 2D geometric method whereby single image slices were analyzed. The moment arm of the flexor digitorum profundus at the third metacarpophalangeal (MCP) joint was measured. Repeating the imaging and measurement process, the 3D tendon excursion method was more reproducible than the 3D geometric method, and both were much more reproducible than the 2D geometric method. The average percent difference of the 3D tendon excursion data was 10%. Data from the 3D geometric and the 3D tendon excursion methods were reasonably similar despite the fact that the analysis was much different. This increased our confidence in the measurements. There was a tendency for moment arm to increase with flexion.

To date, we have reported repeatability of measurements as analyzed by a single operator. We wanted to investigate the variability from one operator to the next. We used 3 different operators on the same set of data. Tendon moment arm measurements were compared (Figure 1.a.i.1). Agreement was excellent, and the average difference was 4%. Another measurement (operator 3 at 50 deg) gave a large deviation on the order of 25% and was not shown. In this case, image quality was poor, and the operator gave an incorrect tendon path because he did not use the sagittal view which greatly reduced errors.

Recall that in the 3D tendon excursion method, moment arm is calculated from $a = \Delta s / \Delta \phi$. Using measurements obtained for Figure 1.a.i.1, we can investigate variability of Δs and $\Delta \phi$. independently. The maximum and average inter-observer differences for Δs are 7% and 4%,

respectively. Values for $\Delta \phi$ are much more repeatable with 3% and 1.2%, respectively. This indicates that most of the error is involved in tendon tracking rather than segmentation of the bones for the angle measurement.

A similar analysis using the 3D geometric method yielded much greater operator variability than that exhibited by the 3D tendon excursion method (not shown).

As described in the last report, we found that moment arms tend to increase with increasing joint angle. In Figure 1.a.i.2, we demonstrate the effect directly on image data. The figure contains carefully reformatted image slices obtained at two joint angles. The dark crosses mark the intersection of the rotational axis with the image slice. On the right as compared to the left image, the moment arm clearly increases because the tendon moves toward the palmar surface and the joint center of rotation moves toward the dorsal surface of the hand.

In Figure 1.a.i.3, 3D tendon paths are plotted in the metacarpal reference frame. Clearly, the increase in the tendon moment arm with flexion angle is explained by a pulling away of the tendon toward the palmar side of the hand and a movement of the joint center of rotation toward the dorsal side of the hand. Similar results are obtained for each of the 4 subjects measured 2 times. As far as we know, this is probably the most direct evidence for increasing tendon moment arm ever presented.

Figure 1.a.i.3 also demonstrates that the beginning point for path length measurements on the metacarpal is sufficiently proximal. That is, all tendon paths overlay nicely indicating that there is no bowstringing at this end. A similar analysis in the frame of the phalanx yields a similar result.

Because of significant differences in moment arm from one subject to another and because moment arm increased with flexion, we recommended patient-specific measurements for target applications in functional neuromuscular stimulation interventions and tendon transfer surgery.

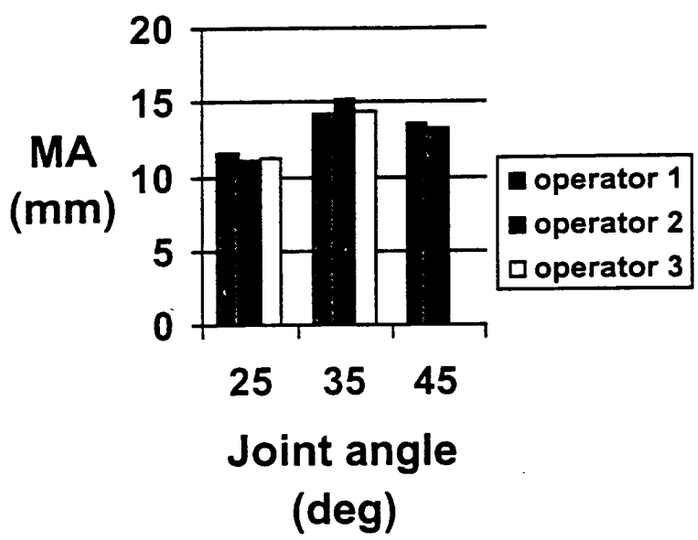

Figure 1.a.i.1 A single image data set (subject RM) is analyzed by 3 different operators using the 3D tendon excursion method. The average percent difference is 4%, and the largest inter-observer difference is < 10%.

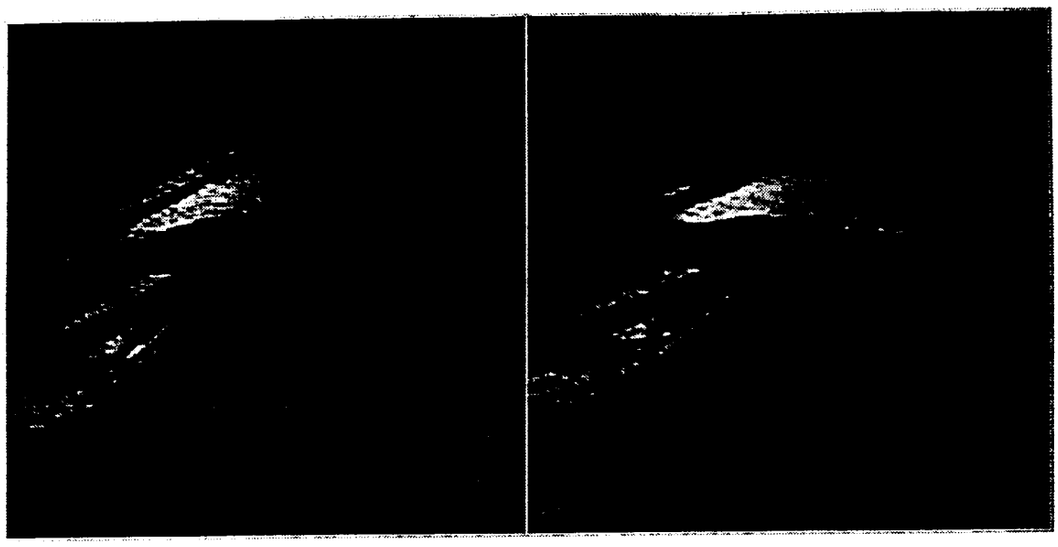

Figure 1.a.i.2 These images show an increase in tendon moment arm with flexion. On the left and right are reformatted image slices taken with the joint angle at 30 deg and 50 deg. respectively. In each case, the dark cross marks the position where the rotational axis intersects the image slice. The distance from the axis of rotation to the tendon is the moment arm, and clearly this increases on the right as compared to the left.

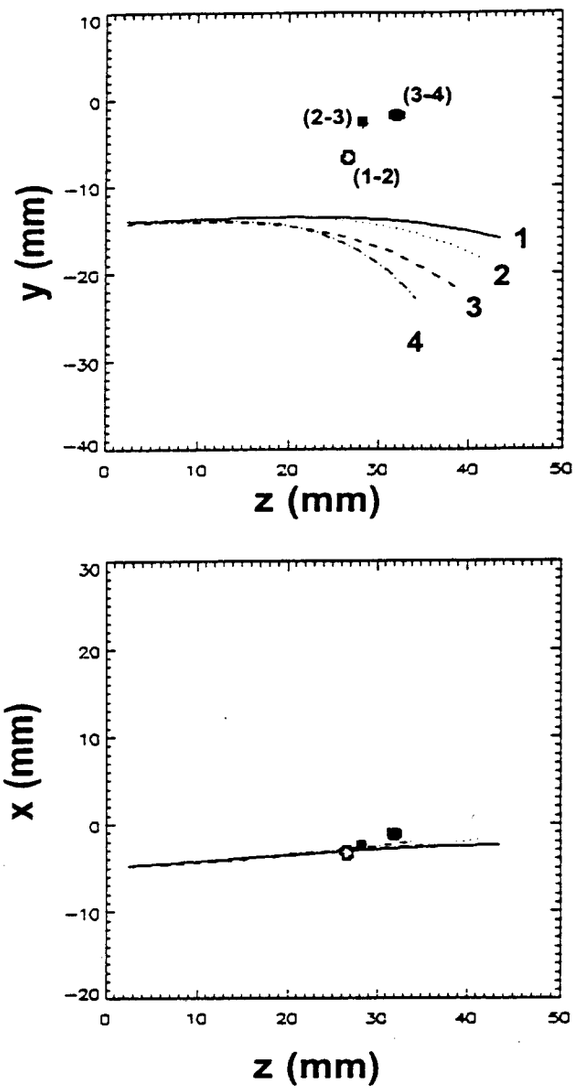

Figure 1.a.i.3 For each of 4 joint angles, tendon paths are transformed into the metacarpal reference coordinate system and plotted. Sagittal and coronal views are plotted top and bottom, respectively. The hand is imaged in 4 positions and tendon paths are labeled accordingly. Intersections of the rotation axis with the tendon plane of motion are also plotted. Each measured axis of rotation requires two image data sets; hence, the open circle marked (1-2) indicates an axis of rotation obtained from data with the joint at positions 1 and 2. In order to correct small inaccuracies in the location of the metacarpal reference, we manually entered small offset values in order to best align the curves. Data are subject JK on day 2.

Plans for next quarter

We will begin to apply the 3D tendon excursion analysis to tendons in the wrist. In addition, we are in the process of documenting and better organizing the programs used to analyze tendon moment arms.

1.a.ii. PASSIVE AND ACTIVE MOMENTS

Purpose

The purpose of this project is to characterize the passive properties of normal and paralyzed hands. This information will be used to determine methods of improving hand grasp and hand posture in FES systems.

Abstract and Report of Progress

During this quarter we began preparation of a manuscript for publication which describes the computer model of the passive moments of the finger (see QPR#6). This model enables us to identify the separate contributions of the extrinsic muscle/tendon units and the tissues of the joint capsule to the total passive moment.

Research efforts during this quarter were focused on the development of the biomechanical model of the hand, as reported in Section 1.b.. We continued to make routine measurements of both active and passive moments with normal and paralyzed subjects.

Plans for Next Quarter

During the next quarter, we will begin to look at methods for making measurements of the passive properties of the distal joints of the fingers. In particular, we are looking at methods of "immobilizing" joints without the use of splints. The basis for this idea is that, by applying the appropriate forces and moments to the tip of the finger, it should be possible to independently control the positions of at least two of the three joints. This may require a splint on the most distal joint (distal interphalangeal), but it would leave both proximal interphalangeal (PIP) and the metacarpalphalangeal (MP) joints free to move. If we can make measurements of the effect of the PIP and DIP joints on MP joint passive properties, then it may be possible to separate the contributions of the flexor digitorum profundus and flexor digitorum superficialis tendons. The initial efforts regarding this idea involve mathematical modeling to determine the accuracy of this method. The results of this modeling will be reported during the next quarter.

1. b. BIOMECHANICAL MODELING: ANALYSIS AND IMPROVEMENT OF GRASP OUTPUT

Abstract

Understanding differences in neuroprosthetic hand function across subjects first requires understanding the differences in the force- and moment-generating capacities of the stimulated muscles. It is important to develop accurate and reliable techniques for quantifying muscle function if we are to analyze and to improve grasp output in neuroprosthesis users. During this quarter, we have continued to take measurements of the isometric elbow extension moment-generating capacity of the stimulated triceps as a function of elbow flexion angle in tetraplegic subjects. We have also begun to evaluate the effects of different stimulation parameters on the measured moment in an attempt to develop an experimental protocol that will yield a consistent, repeatable response of the muscle. In the future, we will use the experimental measurements of isometric strength as a function of joint position to adapt our current biomechanical models to better represent muscle function in tetraplegic subjects.

Objective

The purpose of this project is to use the biomechanical model and the parameters measured for individual neuroprosthesis users to analyze and refine their neuroprosthetic grasp patterns.

Report of Progress

In the past quarter, we have focused on measurement of the isometric moment generated by the electrically stimulated triceps brachii. We are currently in the process of quantifying the degree and sources of variability in our measurements. In addition, we have continued the development of the musculoskeletal

model of the brachioradialis to extensor carpi radialis (Br-ECRB) transfer by digitizing the transferred muscle's path in an anatomical specimen.

Quantifying the Isometric Elbow Extension Moment Generated by the Triceps Brachii

We have measured the isometric moment generated during electrical stimulation of the triceps as a function of elbow flexion angle in two tetraplegic subjects (KRS, JHJ) with implanted neuroprosthetic systems. In both subjects, the triceps was stimulated via an intramuscular electrode implanted in the muscle belly, and the elbow extension moment generated was measured using the elbow moment transducer described previously. In JHJ, the forces and moments generated about the shoulder and elbow during triceps stimulation were also measured using a six-axis force-moment transducer (JR3, Inc.), using the methods described in the previous progress report. In both subjects, repeated measures of the isometric elbow extension moment generated at the same joint position exhibited a high degree of variability (Fig. 1.b.1), making it difficult to quantify differences in elbow extension strength as a function of elbow position. Because this variability in repeated measures was evident using both devices (Fig. 1.b.1B), and because repeated calibrations of the elbow moment transducer are consistent, we do not believe the variability is a function of the measurement device.

In light of the variability in our measurements, and in order to develop appropriate experimental protocols for quantifying strength as a function of joint angle in stimulated muscles, we have begun evaluating different electrical stimulation protocols. Specifically, we are in the process of evaluating the effects of pulse width, frequency, and timing of stimulation on the isometric moment generated in repeated trials. We have quantified the variability in isometric elbow extension moment generated over 16 trials in one joint position (90° elbow flexion) in two tetraplegic subjects (JHJ, CWJ) with implanted

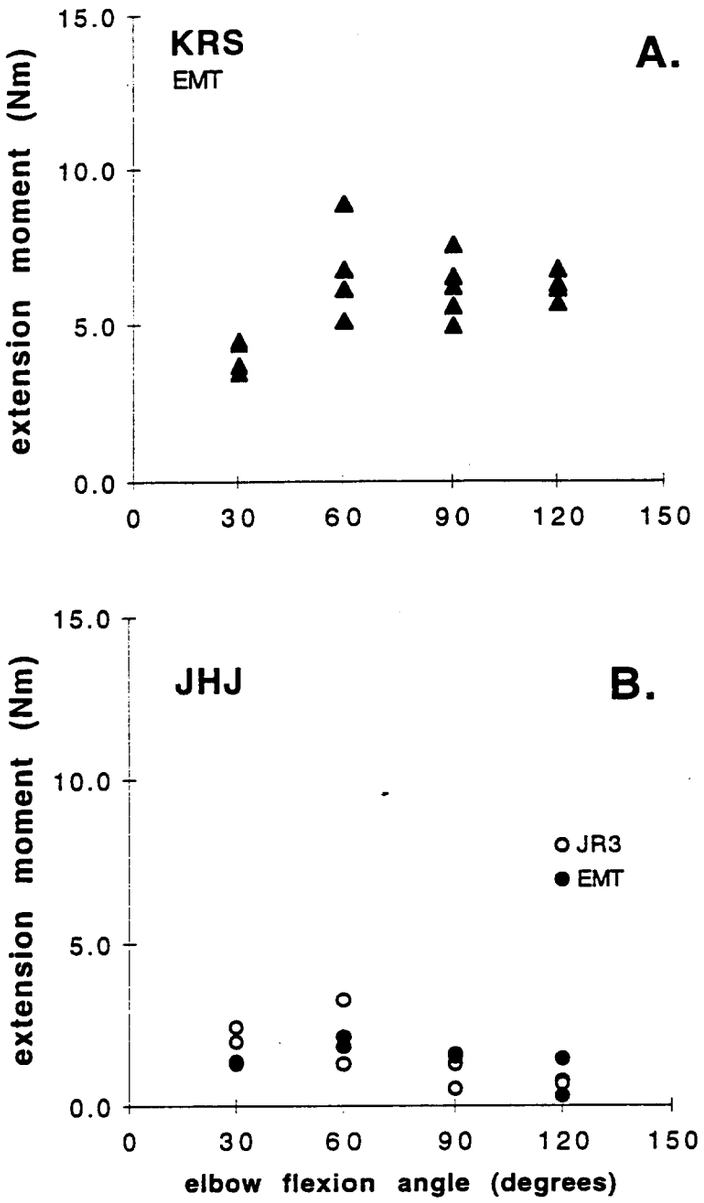

Figure 1.b.1. (A). Isometric elbow extension moment generated by the triceps brachii during functional electrical stimulation as a function of elbow flexion angle in subject KRS. Measurements were taken using the elbow moment transducer (EMT). (B). Isometric elbow extension moment generated by the triceps brachii during functional electrical stimulation as a function of elbow flexion angle in subject JHJ. Open circles show measurements taken with the six-axis force-moment transducer (JR3), and filled circles show measurements from the EMT. Repeated measurements from both KRS and JHJ show a high degree of variability.

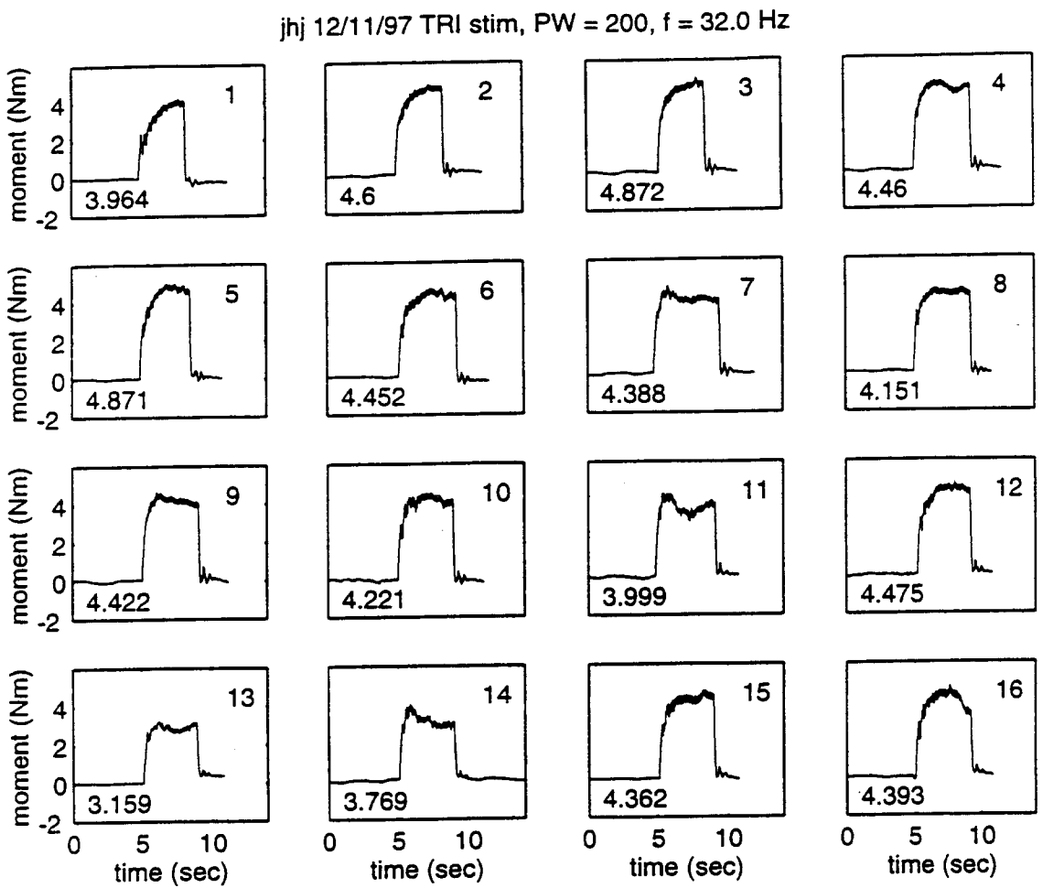

Figure 1.b.2. Isometric elbow extension moment generated by the triceps brachii at 90° elbow flexion during stimulation at the functional pulse width (200 μs) and frequency (12 Hz) over 16 trials in subject JHJ. Measurements were taken using the elbow moment transducer (EMT). Values at the bottom of each plot indicate the maximum isometric moment maintained for at least 0.5s during the trial.

neuroprosthetic systems (Fig. 1.b.2). An individual stimulation trial consists of a pre-stimulation baseline, approximately 3 seconds of triceps stimulation, and a post-stimulation baseline, with 30 seconds rest between consecutive trials. The stimulation parameters are identical across the 16 different trials in a data set. For both subjects, four sets of 16 trials were collected, so that the effects of two different pulse widths and two different stimulation frequencies on the magnitude and time course of the contraction could be tested. The initial stimulation pulse width and frequency were determined based on the individual subject's functional stimulation parameters. The functional pulse width is the maximum pulse width that does not produce spillover to other muscles, and is subject-dependent. The functional frequency is 12 Hz. A second (lower) pulse width was chosen for each subject based on the recruitment curve of the triceps, and a second (higher) frequency was chosen based on the force-frequency relationship of the muscle.

Both frequency and pulse width affected the mean and range of elbow extension moments generated by the triceps over 16 trials (Fig. 1.b.3). Increasing the stimulation frequency increased the mean extension moment produced in both subjects, regardless of stimulation pulse width. Increasing the stimulation frequency *decreased* the range of moments produced at the functional pulse width, but *increased* the range at the lower pulse width in both subjects. As would be expected, decreasing the pulse width decreased the mean extension moment produced in both subjects. The effect of pulse width on the range of the elbow extension moments generated remains unclear. Fatigue did not appear to be an influencing factor in the range of moments produced in a data set in either subject (Fig. 1.b.4). By quantifying the effects of stimulation parameters on the isometric moment generated in repeated trials, we plan to develop an experimental protocol that will allow us to better discriminate between the strength of stimulated muscles at different joint angles.

Digitizing Muscle Paths in Anatomical Specimens

In order to develop a more quantitative model of the Br-ECRB tendon transfer, we digitized muscle-tendon paths on a fresh-frozen cadaver specimen before and after the surgical procedure was performed. After the specimen was thawed, the skin distal to the elbow was removed and steel tacks were inserted along the paths of the extensor carpi radialis brevis and the brachioradialis. The normal anatomical paths of the ECRB and the brachioradialis were digitized before the transfer was performed using an OptoTrak motion analysis system (Northern Digital, Inc.). The camera assembly of the OptoTrak system was mounted on a portable lift, and was positioned above and directly in front of the specimen. The three-dimensional coordinates of the location of a stylus tip were recorded when the stylus, instrumented with LEDs, was positioned on one of the steel tacks inserted along the muscle-tendon paths. The elbow was maintained in full extension, the forearm was placed in the neutral position (0° pronation/supination), and the wrist was maintained in 0° flexion and 0° deviation during digitization. The brachioradialis was then removed from its insertion site on the distal radius, freed from its surrounding fascia over the distal half of the forearm, and transferred to the ECRB. The transferred Br-ECRB path was also digitized using the OptoTrak system. Before and after each path was digitized, anatomical landmarks on the lateral epicondyle of the humerus, the radial and ulnar styloid processes, and the distal ends of the second and third metacarpals were digitized to establish an anatomical reference frame for the upper extremity. The digitized muscle paths will be input into the current biomechanical model of the upper extremity.

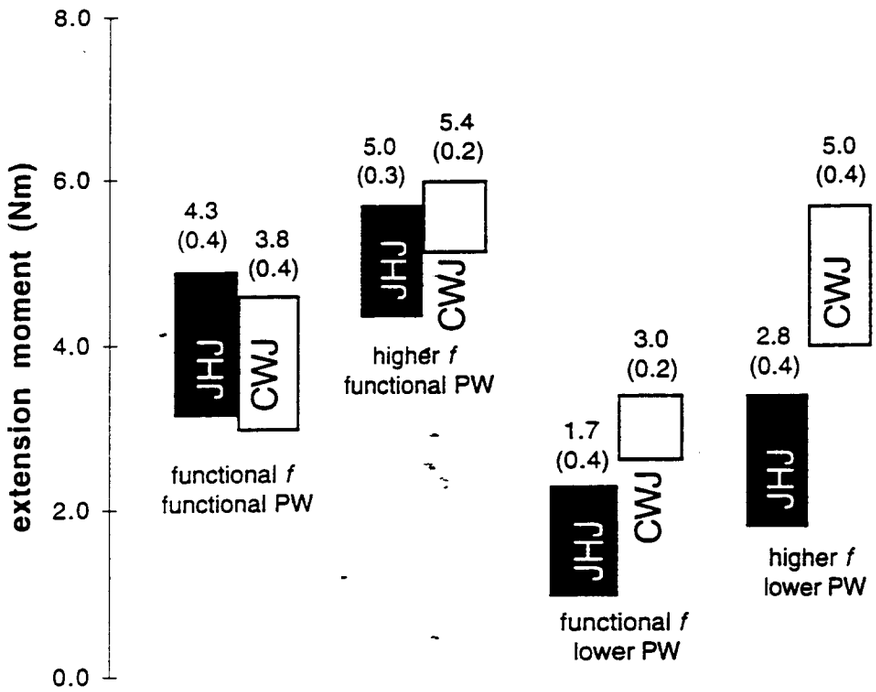

Figure 1.b.3. Range of the isometric elbow extension moment generated by the triceps brachii at 90° elbow flexion during different stimulation protocols over 16 trials in subjects JHJ (filled bars) and CWJ (open bars). Measurements were taken using the elbow moment transducer (EMT). Values above each bar indicate the mean extension moment measured over the 16 trials (standard deviations are in parentheses).

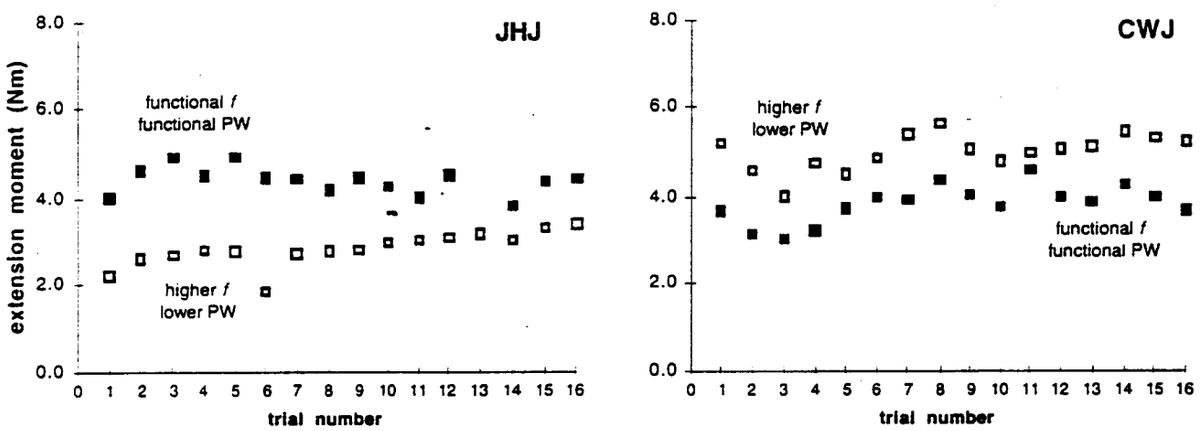

Figure 1.b.4. Maximum isometric elbow extension moment generated by the triceps brachii at 90° elbow flexion during different stimulation protocols over 16 trials in subjects JHJ and CWJ. Measurements were taken using the elbow moment transducer (EMT). Because the variation in the measured moments do not consistently decrease with trial number, fatigue did not play a role in the observed variability between trials.

Plans for Next Quarter

In the next quarter, we plan to continue measurements of the isometric moment generated by the triceps. Further quantification of the degree of variability and fatigue that occurs during repeated trials under different stimulus parameters will be used to develop an experimental protocol that can demonstrate the differences in the elbow extension strength of the triceps at different joint angles and across different subjects. Once the isometric moment-generating capacity of the triceps has been quantified as a function of elbow flexion angle in a number of different subjects, the current biomechanical model of the triceps can be adapted to better represent the function of the triceps in FES users. This will be an important aspect of our analysis of the Br-ECRB transfer because, after transfer, the brachioradialis is still capable of generating a substantial elbow flexion moment. Adequate elbow extension strength may play a crucial role in the success of this procedure.

2. CONTROL OF UPPER EXTREMITY FUNCTION

Our goal in the five projects in this section is to either assess the utility of or test the feasibility of enhancements to the control strategies and algorithms used presently in the CWRU hand neuroprosthesis. Specifically, we will: (1) determine whether a portable system providing sensory feedback and closed-loop control, albeit with awkward sensors, is viable and beneficial outside of the laboratory, (2) determine whether sensory feedback of grasp force or finger span benefits performance in the presence of natural visual cues, (of particular interest will be the ability of subjects to control their grasp output in the presence of trial-to-trial variations normally associated with grasping objects, and in the presence of longer-term variations such as fatigue), (3) demonstrate the viability and utility of improved command-control algorithms designed to take advantage of forthcoming availability of afferent, cortical or electromyographic signals, (4) demonstrate the feasibility of bimanual neuroprostheses, and (5) integrate the control of wrist position with hand grasp.

2. a. HOME EVALUATION OF CLOSED-LOOP CONTROL AND SENSORY FEEDBACK

Abstract

The purpose of this project is to deploy an existing portable hand grasp neuroprosthesis capable of providing closed-loop control and sensory feedback outside of the laboratory. The most promising local candidate for the evaluations is not able to participate, so contingency plans must be formulated.

Purpose

The purpose of this project is to deploy an existing portable hand grasp neuroprosthesis capable of providing closed-loop control and sensory feedback outside of the laboratory. The device is an augmented version of the CWRU hand neuroprosthesis, and was developed and fabricated in the previous contract period. The device utilizes joint angle and force sensors mounted on a glove to provide sensory information, and requires daily support from a field engineer to don and tune. The portable feedback system is not intended as a long term clinical device. Our goal, rather, is to evaluate whether the additional functions provided by this system benefit hand grasp outside of the laboratory, albeit with poor cosmesis and high demands for field support.

Report of Progress

The major obstacle in this project is finding a suitable candidate for implementation and evaluation of the portable closed-loop system who is also willing to participate in the study. We have reduced the external hardware to a minimum for the first phase of the study, from a fully-instrumented sensor glove to a single force sensor worn on the thumb. Preliminary tests of this system in the laboratory with 7 neuroprosthesis users have been encouraging, particularly with subject *L* (see QPR#5), who expressed interest in participating in the at-home evaluations. However, subject *L*'s caregivers were unwilling to participate, even if the study were reduced to simply wearing the PCLS configured for sensory feedback and without the evaluation component (which required daily visits of a rehabilitation engineer).

Plans for Next Quarter

It is clear that this project needs to be re-evaluated carefully. The sensory feedback system has been shown to be feasible, with some evidence of effectiveness. We will formulate a revised strategy for evaluating sensory feedback and/or closed loop control that will satisfy the original objectives of the contract but be better suited to more widespread application. One possibility, as an example, will be to provide force feedback using a small, stand-alone, single-channel, single-sensor device that could be donned by anyone currently using the FreeHand neuroprosthesis nationwide. It would be unrealistic to do at-home evaluations in such subjects, so only subjective data on usage, utility and satisfaction would be collected. Though far from a definitive proof of the effectiveness of sensory feedback, such an evaluation could provide strong motivation to develop sensors and algorithms to augment clinical systems.

2. b. INNOVATIVE METHODS OF CONTROL AND SENSORY FEEDBACK

2. b. i. ASSESSMENT OF SENSORY FEEDBACK IN THE PRESENCE OF VISION

Abstract

The purpose of this project is to develop a method for including realistic visual information while presenting other feedback information simultaneously, and to assess the impact of feedback on grasp performance in the presence of such visual information. In this quarter, a new, more robust method for collecting the video clips was developed and tested. The protocol changes the command increment adaptively to maintain a more constant change in force between successive video frames.

Purpose

The purpose of this project is to develop a method for including realistic visual information while presenting other feedback information simultaneously, and to assess the impact of feedback on grasp performance. Vision may supply enough sensory information to obviate the need for supplemental proprioceptive information via electrocutaneous stimulation. Therefore, it is essential to quantify the relative contributions of both sources of information.

Report of Progress

As described in the last report, the video simulation system is functional, but the video playback could be erratic in certain regions of the command range where force increased rapidly for a small change in command (i.e., in steep regions of the recruitment function). To review, video clips are collected in the existing system by ramping the command to the neuroprosthesis from 0-100% via a computer external to the neuroprosthesis control unit, and collecting grasp force information and videotaping the hand simultaneously. The clips are played back, then, by reading a command signal from a shoulder transducer and then recalling the video frame corresponding to that command. We can imagine increasing the command at a constant rate of ∂C per sample during the data collection, producing force increments ∂F determined by the slope of the recruitment function. As shown in Fig. 2.b.i.1(A), such fixed-interval sampling will produce large changes in the output if the recruitment function is steep. We have produced adequate video clips using such an algorithm, but at the expense of a very slow ramp rate and very large video files. It is more efficient to choose the command increment for the next step based on the rate at which force changed on immediately preceding steps; and, to increment the command in such a way that each step advances the output some fixed length ∂S along the recruitment curve rather than a fixed ∂F or ∂C. This latter rule, illustrated in Fig. 2.b.i.1(B), insures that neither the command increment nor the force increment exceed ∂S. The algorithm also allows the data collection to proceed at a constant rate, $\partial S/\partial t$, when the force output is not changing. Put another way, the algorithm keeps the density of video frames constant along the length of the recruitment function, producing efficient but smooth video clips. The actual selection of the command step for a given sample is accomplished by fitting N preceding points with a function, extrapolating that function a distance ∂S, and then calculating the commensurate command step ∂C .

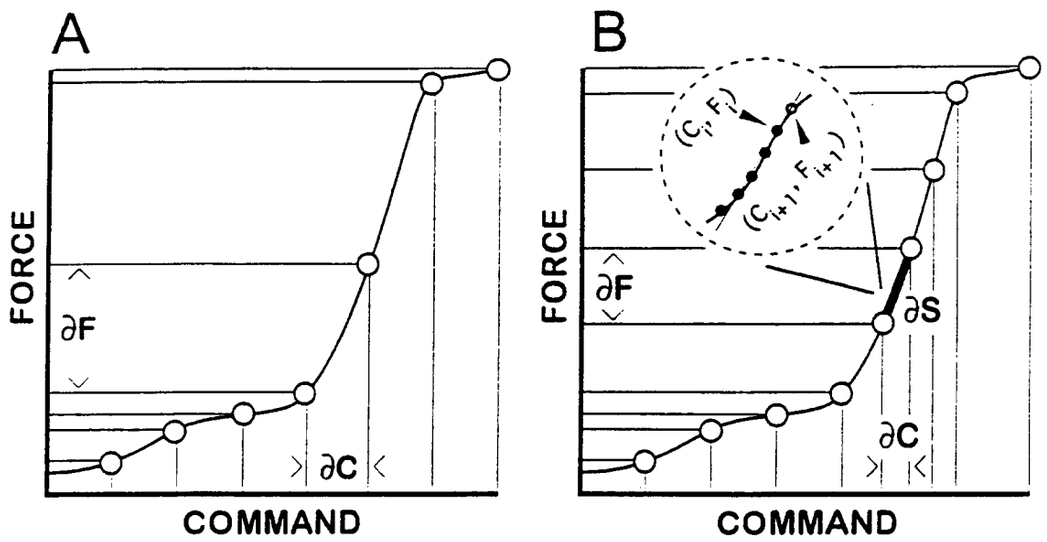

Fig. 2.b.i.1 Illustration of command ramp algorithms for collecting video clips. The algorithm in **A** uses a fixed command increment between each cycle, resulting in large force increments in regions of steep recruitment. The adaptive algorithm in **B** uses the rate of force change over some previous number of samples (see inset) to estimate the next appropriate command so that each command increment moves a fixed distance ∂S along the recruitment curve.

We have implemented and tested this algorithm with one neuroprosthesis user to demonstrate its feasibility. We used a linear least-squares fit to 5 points to extrapolate forward to the next command value. If the fit has a slope b, then the command increment ∂C is equal to: $\partial C = \partial S / \sqrt{1+b^2}$. The length increment ∂S was selected by dividing the length (line integral) of a representative recruitment function by the total number of samples (3000). The latter number was equal to the number of samples (10) collected for each video frame (300). The command and force values are plotted as a function of time in Fig. 2.b.i.2. Note that overall the command increased with a fairly constant rate. However, in the regions where the force increases rapidly, the command rate declines, allowing more video frames to be collected over this force range. The video clips collected using the adaptive command algorithm are smooth and produce natural-looking movements when played back with a shoulder controller. The new clips rival the best clips collected previously that used very slow command ramps — but are significantly smaller.

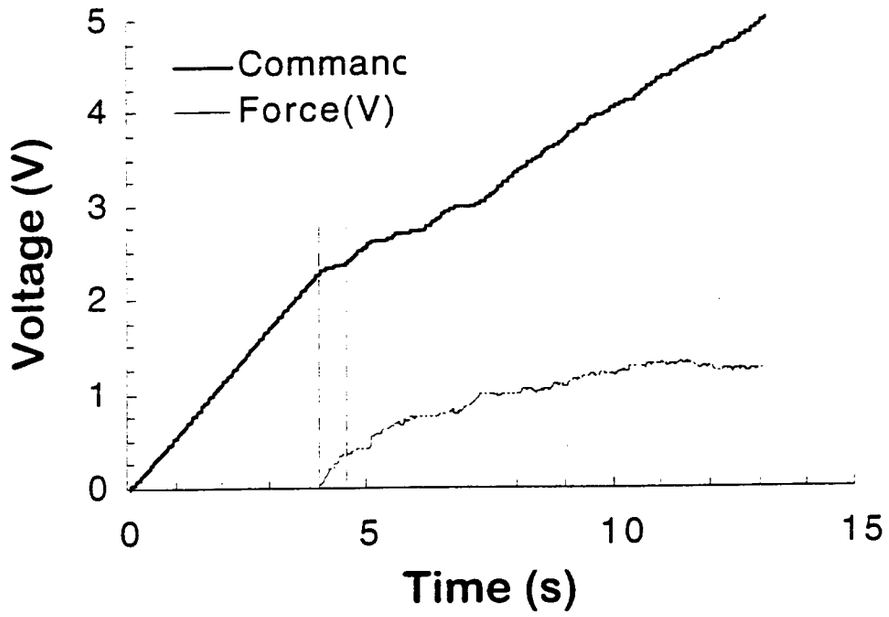

Fig. 2.b.i.2 Plots of command ramp and force output for one video clip collected using the adaptive algorithm. Note that at the beginning the command increases at a constant rate since the force is not changing. However, the command rate decreases as soon as the force increases (e.g. between the dashed lines). The result is a relatively constant video frame density over the entire length of the recruitment function, rather than over the range of commands or forces.

We are also developing an evaluation platform that will allow us to optimize the algorithm parameters;. In the present case, the only parameter is the incremental length ∂S. Although we estimated ∂S initially using a recruitment curve and a desired number of frames, the algorithm will actually use its assigned ∂S and consume as many frames as it requires to ramp from 0-100% command. Therefore, it is highly desirable to find an independent estimate of the best ∂S. We will do so empirically with a simulator that consists of a parent video clip that was collected using an extremely slow command ramp (100 sec). The sampling algorithm will be applied to this parent video clip to select out a sub-sample of the video frames, and then that subset will be played back and assessed for fidelity and smoothness. We will generate video clips as a function of ∂S, and identify the optimal value (or the largest value in a range of values with indistinguishable results) based on video quality. Using a single parent video will enhance the discriminability of quality by permitting direct AB comparisons of the identical scene.

Plans for Next Quarter

We will complete the evaluator based on the parent video clip, and use it to identify an optimal increment length. Then, video clips will be collected from several neuroprosthesis users and be used in the evaluations of sensory feedback and control strategies.

2. b. ii. INNOVATIVE METHODS OF COMMAND CONTROL

Abstract

There was no progress in this area during the past quarter.

Purpose

The purpose of this project is to improve the function of the upper extremity hand grasp neuroprosthesis by improving user command control. We are specifically interested in designing

algorithms that can take advantage of promising developments in (and forthcoming availability of) alternative command signal sources such as EMG, and afferent and cortical recordings. The specific objectives are to identify and evaluate alternative sources of logical command control signals, to develop new hand grasp command control algorithms, to evaluate the performance of new command control sources and algorithms with a computer-based video simulator, and to evaluate neuroprosthesis user performance with the most promising hand grasp controllers and command control sources.

Plans for Next Quarter

In the next quarter we will continue analysis of the optimum parameters for contact detection. We will also initiate command control algorithm evaluation using the video simulator (see C.2.b.i).

2. b. iii. INCREASING WORKSPACE AND REPERTOIRE WITH BIMANUAL HAND GRASP

Abstract

Strategies for utilizing surface EEG mu rhythms are under investigation. A collaborative relationship has been established with a leading research team in this field, lead by Dr. Jonathan Wolpaw at the Wadsworth Center for Labs and Research in Albany, NY. Using data derived from able-bodied individuals supplied to us by this team, a possible command control strategy was derived for using the EEG signal to operate a neuroprosthesis. This algorithm uses high levels of mu rhythm activity to operate the system state (on/off) and the lower levels of activity to generate a proportional control signal to generate hand opening and closing. This algorithm has been tested out on data collected from two able bodied subjects with varying degrees of experience in controlling the EEG signal, but with a high degree of accuracy. The results of this analysis are presented.

Purpose

The objective of this study is to extend the functional capabilities of the person who has sustained spinal cord injury and has tetraplegia at the C5 and C6 level by providing the ability to grasp and release with both hands. As an important functional complement, we will also provide improved finger extension in one or both hands by implantation and stimulation of the intrinsic finger muscles. Bimanual grasp is expected to provide these individuals with the ability to perform over a greater working volume, to perform more tasks more efficiently than they can with a single neuroprosthesis, and to perform tasks they cannot do at all unimanually.

Report of progress

In this quarter, preliminary investigation was conducted on using the EEG signal, as recorded by the brain-computer interface (BCI) system developed by Dr. Wolpaw and his colleagues (as discussed in QPR #5), to operate a neuroprosthesis. Data was provided by Dr. Wolpaw on five able-bodied subjects, all with varying degrees of control over the EEG signal and with varying degrees of experience in using the signal to control cursor movement. For each of the subjects, data on two to four trials was provided so that an analysis of the changes in the EEG signal over time could be conducted. At this time, a detailed analysis has been conducted on two out of the five subjects. The results from this analysis are presented below. From these preliminary results, it has been determined that if the quality of the signal which has been recorded from the able-bodied subjects is the same in persons with a spinal cord injury, it may be feasible to use the EEG signal to control either the operating state of the system (on/off/lock), the degree of hand opening/closing, or both.

The signal which is used to operate the movement of the computer cursor for one of the subjects is shown in Figure 2.b.iii.1a. This signal is derived from the spectral analysis of the EEG signal in the 12-15 Hz range (mu rhythm) , recorded over the motor cortex at locations C3/C4 (on the 10-20 system). The spectral analysis is accomplished using an autoregressive moving average (ARMA) method, and the power at the 12-15 Hz band is calculated every 200 ms. The peaks in the figure correspond to the subject generating the command to move the cursor upwards, while the valleys, in most cases, correspond to the

command to move the cursor downwards. The resting level for the subject in this example is approximately -30 microvolts.

As seen in Figure 2.b.iii.1a, the signal that is used for cursor movement is extremely noisy. This signal would be ineffective in providing a high degree of control of the neuroprosthesis. At best, this signal could only be used as an on/off signal using high and low level threshold detection. Initially, low pass filtering using Butterworth and Chebyshev type filters to decrease the noise level was used, but this introduced a phase delay. This delay was on the order of 200-500 ms, which was unacceptable for use in a neuroprosthesis when a delay of less than 200 ms between the time the signal is generated and the system responds is believed maximal. Therefore, to provide the necessary filtering without introducing a phase delay, the adaptive step size filter which has been developed in our laboratories for use in reducing noise in electromyographic signals was used. This filter functions as an N-point smoother without introducing the phase delay inherent with other low pass filtering techniques. The results of using the adaptive step size filter are shown in Figure 2.b.iii.1b. This is the same signal as represented in Figure 2.b.iii.1a, but much of the noise content has been removed while maintaining the important features of the signal and the same time course.

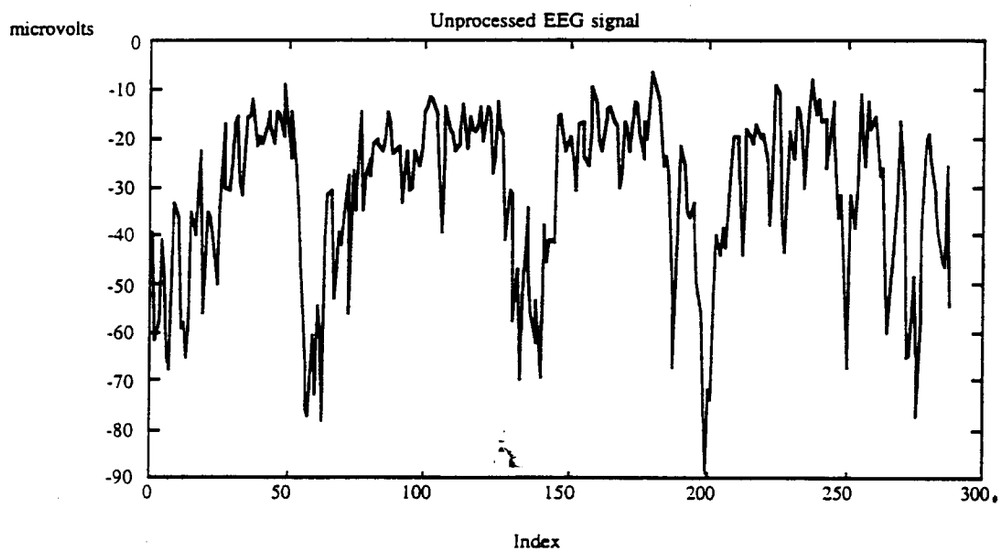

Fig. 2.b.iii.1a Unprocessed EEG signal used for cursor control